Heat transfer between rotating spheres and flowing power-law fluids with suction and injection

C. Kleinstreuer and T.-Y. Wang
Department of Mechanical and Aerospace Engineering,
North Carolina State University, Raleigh, NC 27695-7910, USA

Received November 1987

Steady laminar forced convection of non-Newtonian fluids past rotating spheres with permeable walls has been analyzed. New coordinate transformations are used to reduce the streamwise dependence of the coupled nonlinear boundary layer equations, simplifying the numerical solution procedure. The effects of the type of power-law fluid on the local skin friction coefficient and heat transfer coefficient are determined. As expected, both increase with increasing body rotation, while fluid injection decreases them and fluid withdrawal increases them. The effect of the mass transfer parameter on the local heat transfer group is significant for power-law fluids with large Prandtl numbers. The angle of boundary layer separation decreases with increasing index number of the power-law viscosity model.

Keywords: forced convection heat/mass transfer; power-law fluids; rotating, porous sphere; non-Newtonian fluid

Introduction

The analysis of a spinning axisymmetric body in a non-isothermal flow field is of interest in rotary machine design, including transpiration cooling, moving or reentering projectile behavior, wire or fiber coating, and foodstuff processing. Some of these applications involve non-Newtonian fluids which can be approximated with the power-law viscosity model. The introduction of the additional nonlinearity into the momentum equation excludes the Mangler transformation, typically used in the solution procedure for axisymmetric boundary layer flow problems. Body rotation may enhance convection heat transfer because centrifugal forces push the fluid near the surface outward, which is then replaced by fluid of a different temperature. If the wall of the submerged body is porous or perforated, fluid at a prescribed temperature can be injected into the boundary layer (blowing) or fluid at the wall surface can be withdrawn (suction). These additional mass transfer processes may measurably alter the local skin friction and heat transfer coefficients.

Simplified forms of the present system have been extensively analyzed in the past. For example, Hoskin[1] calculated the boundary layer parameters for flow past a rotating sphere using the Blasius-series technique. Koh and Price[2] considered forced nonisothermal flow past a rotating cone, and Chao and Greif[3] assumed a quadratic velocity profile to study forced convection heat transfer over rotating bodies with arbitrary surface temperature. Lee *et al.*[4] used a Merk series expansion to solve the same problem[3] for a wider range of Prandtl numbers and body speeds. Lien *et al.*[5] extended the previous paper[4] to analyze the effect of injection and suction of fluid at the body surface. Tsay and Chou[6] studied forced convection heat transfer between a rotating disk and a power-law fluid. Considering a step change in temperature, the instant-local similarity method was used to solve the problem. With the exception of their work,[6] in all previous investigations the fluid was Newtonian and somewhat restrictive series expansions were employed to solve particular boundary layer equations.

The present analysis concentrates on steady laminar forced convection of a power-law fluid past a permeable, rotating axisymmetric body. The four describing partial differential equations are transformed to three coupled nonlinear differential equations which contain partial derivatives in the streamwise direction only. An implicit finite difference scheme is used to solve the reduced system of equations. The example of a rotating permeable sphere is given to illustrate the effects of the power-law viscosity index and the generalized non-Newtonian Prandtl number on the local skin friction coefficient and Nusselt number.

Analysis

Modelling equations for an axisymmetric body

Consider steady laminar axisymmetric boundary layer flow of a power-law fluid past a spinning, permeable body at constant wall temperature. The axis of rotation is parallel to the free-stream velocity (Figure 1). The nonrotating orthogonal coordinates x and y are measured from the forward stagnation point along the body surface and outward normal to the wall, respectively. The velocity component u is in the x direction, v is in the y direction, and w is the transverse velocity due to the body spin. Neglecting wake effects and assuming constant properties, the describing equations are[4,7]

$$\frac{\partial}{\partial x}(ru)+\frac{\partial}{\partial y}(rv)=0 \tag{1}$$

$$u\frac{\partial u}{\partial x}+v\frac{\partial u}{\partial y}-\frac{w^2}{r}\frac{\mathrm{d}r}{\mathrm{d}x}=u_e\frac{\mathrm{d}u_e}{\mathrm{d}x}+\frac{K}{\rho}\frac{\partial}{\partial y}\left[\left|\frac{\partial u}{\partial y}\right|^{n-1}\frac{\partial u}{\partial y}\right] \tag{2}$$

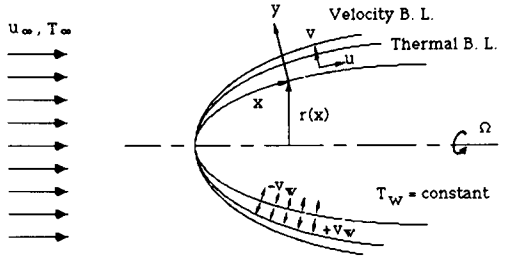

Figure 1 System schematic

$$u\frac{\partial w}{\partial x}+v\frac{\partial w}{\partial y}+\frac{uw}{r}\frac{\mathrm{d}r}{\mathrm{d}x}=\frac{K}{\rho}\frac{\partial}{\partial y}\left[\left|\frac{\partial w}{\partial y}\right|^{n-1}\frac{\partial w}{\partial y}\right] \tag{3}$$

$$u\frac{\partial T}{\partial x}+v\frac{\partial T}{\partial y}=\alpha\frac{\partial^2 T}{\partial y^2} \tag{4}$$

subject to the boundary conditions

$$\begin{aligned}&\text{at } y=0: \quad u=0,\quad v=\pm v_w,\quad w=r\Omega,\quad \text{and}\quad T=T_w\\&\text{at } y\to\infty: \quad u=u_e(x),\quad w=0,\quad \text{and}\quad T=T_\infty\end{aligned} \tag{5}$$

where v_w is the wall velocity due to blowing or suction.

The system of equations can be reduced using the stream function approach

$$u=\frac{1}{r}\frac{\partial\psi}{\partial y}\quad\text{and}\quad v=-\frac{1}{r}\frac{\partial\psi}{\partial x} \tag{6a, b}$$

and the transformations

$$\xi=\frac{x}{L},\qquad \eta=\left(\frac{\mathrm{Re}}{\xi}\right)^{1/(n+1)}\left(\frac{u_e}{u_\infty}\right)^{(2-n)/(n+1)}\frac{y}{L} \tag{7a, b}$$

$$\psi=rLu_\infty\left(\frac{\xi}{\mathrm{Re}}\right)^{1/(n+1)}\left(\frac{u_\infty}{u_e}\right)^{(1-2n)/(n+1)}F(\xi,\eta)-\int_0^x rv_w\,\mathrm{d}x \tag{7c}$$

$$\theta(\xi,\eta)=\frac{T-T_\infty}{T_w-T_\infty}\quad\text{and}\quad g(\xi,\eta)=\frac{w}{r\Omega} \tag{7d, e}$$

where

$$\mathrm{Re}=\frac{\rho u_\infty^{2-n}L^n}{K}$$

is the generalized Reynolds number, with L being a characteristic length of the body.

As a result, the continuity equation is automatically satisfied, and the momentum equations and the energy equation are transformed to

$$\begin{aligned}&(|F''|^{n-1}F'')'+\gamma(\xi)FF''+\Lambda(\xi)(1-F'^2)\\&\quad+C(\xi)g^2-\mathrm{MP}D(\xi)F''=\xi\left[F'\frac{\partial F'}{\partial\xi}-F''\frac{\partial F}{\partial\xi}\right]\end{aligned} \tag{8}$$

$$\begin{aligned}&G(\xi)(|g'|^{n-1}g')'+\gamma(\xi)g'F-H(\xi)gF'-\mathrm{MP}D(\xi)g'\\&\quad=\xi\left[F'\frac{\partial g}{\partial\xi}-g'\frac{\partial F}{\partial\xi}\right]\end{aligned} \tag{9}$$

and

$$\frac{E(\xi)}{\mathrm{Pr}}\theta''+\gamma(\xi)\theta'F-\mathrm{MP}D(\xi)\theta'=\xi\left[F'\frac{\partial\theta}{\partial\xi}-\theta'\frac{\partial F}{\partial\xi}\right] \tag{10}$$

where

$$\Lambda(\xi)=\frac{\xi}{u_e}\frac{\mathrm{d}u_e}{\mathrm{d}\xi} \tag{11a}$$

$$\gamma(\xi)=\frac{1}{n+1}+\frac{2n-1}{n+1}\Lambda+\frac{\xi}{r}\frac{\mathrm{d}r}{\mathrm{d}\xi} \tag{11b}$$

$$C(\xi)=\frac{\xi}{r}\frac{\mathrm{d}r}{\mathrm{d}\xi}\mathrm{BP}\left(\frac{r/L}{u_e/u_\infty}\right)^2 \tag{11c}$$

$$D(\xi)=\xi^{n/(n+1)}\left(\frac{u_e}{u_\infty}\right)^{(1-2n)/(n+1)} \tag{11d}$$

$$E(\xi)=\left(\frac{u_e}{u_\infty}\right)^{3(1-n)/(n+1)}\xi^{(n-1)/(n+1)} \tag{11e}$$

$$G(\xi)=\left(\mathrm{BP}^{1/2}\frac{r/L}{u_e/u_\infty}\right)^{n-1} \tag{11f}$$

Notation

BP	Rotation parameter, $\mathrm{BP}=(L\Omega/u_\infty)^2$
BP*	Rotation parameter, $\mathrm{BP}^*=\mathrm{BP}/2.25$
BP**	Rotation parameter, $\mathrm{BP}^{**}=(R\Omega/u_e)^2$
c_f	Local skin friction coefficient
F	Dimensionless stream function
g	Dimensionless velocity
h	Local heat transfer coefficient
K	Fluid consistency index for power-law fluid
k	Thermal conductivity
L	Characteristic length of rotating body
MP	Mass transfer parameter
Nu	Local Nusselt number
n	Index of power-law viscosity model
Pr	Generalized Prandtl number
Re	Generalized Reynolds number
R	Radius of sphere
r	Distance from a point on the surface to the axis of symmetry
T	Temperature
u	Velocity component in x direction
v	Velocity component in y direction
w	Transverse velocity component
x	Streamwise coordinate along the body surface measured from the forward stagnation point
y	Coordinate normal to the surface

Greek Symbols

α	Thermal diffusivity
η	Dimensionless coordinate
θ	Dimensionless temperature
ρ	Density of fluid
τ	Shear stress
ξ	Dimensionless coordinate
ψ	Stream function
Ω	Angular velocity
ϕ	Angle of sphere

Subscripts

e	Boundary layer edge condition
∞	Ambient condition
w	Wall condition

$$H(\xi)=2\frac{\xi}{r}\frac{\mathrm{d}r}{\mathrm{d}\xi} \tag{11g}$$

The rotation parameter BP is defined as

$$\mathrm{BP}=\left(\frac{L\Omega}{u_\infty}\right)^2 \tag{12a}$$

and the mass transfer or blowing/suction parameter MP is defined as

$$\mathrm{MP}=\pm\frac{v_w}{u_\infty}\mathrm{Re}^{1/(n+1)} \tag{12b}$$

The generalized Prandtl number is

$$\mathrm{Pr}=\frac{u_\infty L}{\alpha}\mathrm{Re}^{-2/(n+1)} \tag{12c}$$

The corresponding boundary conditions are

$$\begin{aligned}&\text{at } \eta=0: \quad F'=F=0 \quad \text{and} \quad g=\theta=1\\ &\text{at } \eta\to\infty: \quad F'=1, \quad g=0, \quad \text{and} \quad \theta=0\end{aligned} \tag{13a, b}$$

With the definition of the local skin friction coefficient

$$c_f=\frac{\tau_w}{\frac{1}{2}\rho u_\infty^2}$$

a dimensionless skin friction group, SFG, can be formed as

$$\mathrm{SFG}\equiv\tfrac{1}{2}c_f\,\mathrm{Re}^{1/(n+1)}=\xi^{-n/(n+1)}\left(\frac{u_e}{u_\infty}\right)^{3n/(n+1)}[F''(\xi,0)]^n \tag{14}$$

Similarly, with the local Nusselt number as

$$\mathrm{Nu}=\frac{hL}{k}$$

a dimensionless heat transfer group, HTG, can be formed as

$$\mathrm{HTG}\equiv\mathrm{Nu}\,\mathrm{Re}^{-1/(n+1)}=-\xi^{-1/(n+1)}\left(\frac{u_e}{u_\infty}\right)^{(2-n)/(n+1)}\theta'(\xi,0) \tag{15}$$

For a specific problem solution, the shape of the body, $r(x)$, and the outer flow distribution $u_e(x)/u_\infty$ have to be known.

Application to a rotating sphere

For a sphere, $r(x)=R\sin(x/R)$, where R is the radius of the sphere which corresponds to the characteristic length L. Laminar boundary layers can be assumed for Reynolds numbers based on the sphere diameter up to $\mathrm{Re}_d\approx 200$, although vortex shedding might occur already at $\mathrm{Re}_d\approx 130$. From potential flow theory

$$\frac{u_e}{u_\infty}=\tfrac{3}{2}\sin\left(\frac{x}{R}\right) \tag{16a}$$

which is assumed here in order to be able to compare our results with previously published case studies. Alternatively, an empirical expression for u_e/u_∞ could be employed; for example,[7]

$$\frac{u_e}{u_\infty}=1.5\xi-0.4371\xi^3+0.1481\xi^5-0.0423\xi^7 \tag{16b}$$

With $r(x)$, u_e/u_∞, and L identified, the coefficients (11a)–(11g) take on the form

$$\begin{aligned}\Lambda&=\xi\cot\xi\\ \gamma&=\frac{1}{n+1}+\frac{2n-1}{n+1}\Lambda+\xi\cot\xi\\ C&=\tfrac{4}{9}\xi\mathrm{BP}\cot\xi\\ D&=\xi^{n/(n+1)}(\tfrac{3}{2}\sin\xi)^{(1-2n)/(n+1)}\\ E&=\xi^{(n-1)/(n+1)}(\tfrac{3}{2}\sin\xi)^{3(1-n)/(n+1)}\\ G&=(\tfrac{2}{3}\mathrm{BP}^{1/2})^{n-1}\\ H&=2\xi\cot\xi\end{aligned} \tag{17a–g}$$

Numerical solution

The modeling equations, Equations 8 to 10, with the appropriate coefficients for the rotating sphere case (17a–g) were solved numerically using the two-point finite difference method outlined in Cebeci and Bradshaw.[8] A nonuniform mesh with a very fine grid spacing near the stagnation point was selected to obtain accurate velocity and temperature profiles. A total of 121 nodal points in the ξ direction and 144 grid points in the η direction were necessary in order to achieve mesh density independence of the results.

Results and discussio

In order to verify the accuracy of our computer simulation model, we compared our results with accepted data sets for an impermeable, rotating disk[2] and a sphere[1,4,5] in a uniform stream of a Newtonian fluid. Excellent agreement for HTG values (cf. Equation 15) obtained at different Prandtl numbers and disk speeds is shown in Table 1. A consistently good data match was also achieved for the rotating sphere case when the local skin friction group (SFG values) and the heat transfer group (HTG values) were compared as given in Tables 2 and 3, respectively. Figures 2 and 3 show practically the identical graphs as given by Lien *et al.*[5] as well as the impact of the edge velocity distribution on the wall parameters SFG and HTG. For the following graphs, Equation 16a has been used.

Figures 4 and 5 depict the SFG and HTG distributions for different types of fluids at Pr = 100 flowing past a heated, impermeable sphere rotating at BP = 1.0 or 10.0. As expected,

Table 1 Data comparison of $\mathrm{HTG}=\mathrm{Nu}/\mathrm{Re}^{1/(n+1)}$ for a rotating disk; MP = 0 and $n=1$

	Pr = 0.7		Pr = 1.0		Pr = 10.0	
BP**	Koh & Price (1967)	Present method	Koh & Price (1967)	Present method	Koh & Price (1967)	Present method
0.0	0.6653	0.6653	0.7621	0.7621	1.750	1.7517
0.6	0.6755	0.6753	0.7750	0.7748	1.801	1.7972
1.0	0.6818	0.6816	0.7830	0.7828	1.829	1.8256
4.0	0.7220	0.7222	0.8336	0.8339	2.003	2.0049
5.0	0.7338	0.7337	0.8485	0.8484	2.058	2.0551
10.0	0.7819	0.7823	0.9092	0.9096	2.261	2.2627
15.0	0.8190	0.8210	0.9565	0.9584	2.430	2.4248

the skin friction coefficient is larger at high rotation and reaches at $\xi = 0.96$, i.e., near $\phi = 55°$, a maximum before dropping eventually to zero at the point of boundary layer separation. At very low speeds, BP $\leqslant 1.0$, the effect of the type of power-law fluid on SFG is less pronounced (cf. Figure 4). Computer experiments showed that the angle of boundary layer separation, measured from the forward stagnation point, decreases with increasing index of the power-law viscosity model. This trend is indicated in Figure 4. A subtle effect of rotation is the fact that dilatant fluids ($n > 1.0$) generate larger SFG values in the vicinity of $c_{f,max}$ than do pseudoplastics. This behavior depends upon the $u_e/u_\infty(\xi)$ approximation used. For example, for stationary bodies the SFG for pseudoplastics is consistently higher than for dilatant fluids when an empirical outer flow velocity function is employed.[7] Figure 5 shows the unique HTG distributions for Newtonian and power-law fluids flowing past a heated, spinning sphere. An increase in angular velocity enhances the heat transfer moderately. The contrasting behavior of the two types of power-law fluids near the stagnation point can be explained with Equation 15. For small ξ, we approximate u_e/u_∞ (cf. Equation 16) and obtain

$$\text{HTG} \sim \xi^{(1-n)/(n+1)}\theta'(\xi, 0)$$

Table 2 Comparison of SFG $= \frac{1}{2}c_f \text{Re}^{1/(n+1)}$ for a rotating sphere; MP $= 0$, $n = 1$

BP*	X/R	Hoskin (1955)	Lee *et al.* (1978)	Lien *et al.* (1986)	Present method
	0.474	1.2497	1.2496	1.2499	1.2499
	0.951	1.8402	1.8403	1.8400	1.8400
1	1.215	1.7203	1.7207	1.7185	1.7184
	1.374	1.4783	1.4780	1.4732	1.4727
	1.486	1.2336	1.2269	1.2173	1.2171
	0.474	1.8170	1.8170	1.8182	1.8174
	0.951	2.6359	2.6362	2.6366	2.6356
4	1.215	2.4031	2.4023	2.3990	2.3979
	1.374	1.9953	1.9892	1.9786	1.9769
	1.486	1.5876	1.5644	1.5373	1.5361
	0.474	2.8165	2.8166	2.8196	2.8172
	0.951	4.0440	4.0444	4.0462	4.0432
10	1.215	3.6218	3.6186	3.6133	3.6100
	1.374	2.9312	2.9144	2.8930	2.8888
	1.486	2.2451	2.1897	2.1313	2.1277

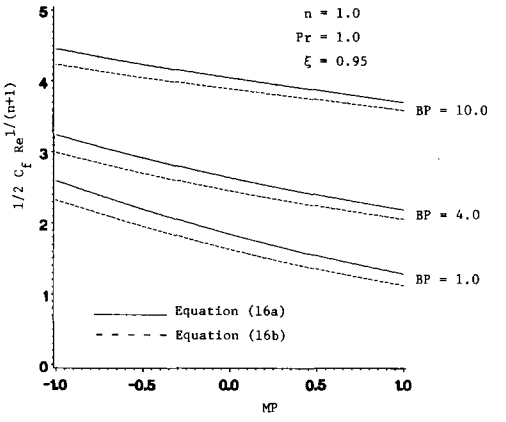

Figure 2 Skin friction group as a function of mass transfer parameter with the effects of sphere rotation and edge velocity distribution

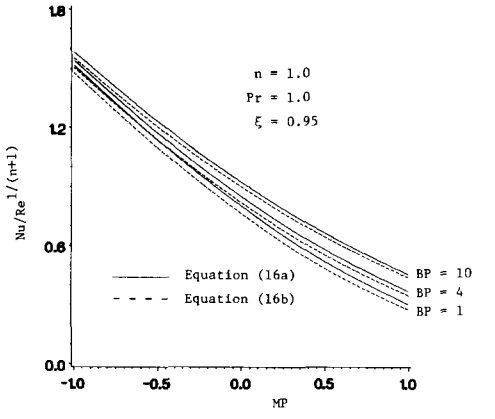

Figure 3 Heat transfer group as a function of mass transfer parameter with the effects of sphere rotation and edge velocity distribution

Table 3 Data comparisons of HTG $= \text{Nu}/\text{Re}^{1/(n+1)}$ for a rotating sphere; MP $= 0$, $n = 1$

		BP* = 1.0				BP* = 10			
Pr	X/R	Hoskin (1955)	Lee *et al.* (1978)	Lien *et al.* (1986)	Present method	Hoskin (1955)	Lee *et al.* (1978)	Lien *et al.* (1986)	Present method
	0.0	0.9589	0.9588	0.9586	0.9587	1.0914	1.1141	1.1142	1.1140
	0.951	0.7792	0.7998	0.7993	0.7994	0.9264	0.9218	0.9215	0.9214
1	1.219	0.7064	0.6961	0.6966	0.6965	0.8042	0.7904	0.7924	0.7921
	1.374	0.6275	0.6171	0.6195	0.6194	0.7223	0.6825	0.6902	0.6895
	1.486	0.5557	0.5510	0.5559	0.5556	0.5905	0.5776	0.5982	0.5972
	0.0	2.2364	2.2363	2.2359	2.2359	2.7635	2.7718	2.7701	2.7713
	0.951	1.8571	1.8520	1.8513	1.8510	2.2722	2.2695	2.2684	2.2684
10	1.215	1.6029	1.5994	1.6004	1.5993	1.9363	1.9234	1.9278	1.9253
	1.374	1.4173	1.4084	1.4102	1.4081	1.6640	1.6434	1.6543	1.6489
	1.486	1.2600	1.2551	1.2511	1.2482	1.4180	1.3912	1.4004	1.3957
	0.0	—	4.9878	4.9947	4.9864	—	6.3845	6.3848	6.3823
	0.951	—	4.1151	4.1238	4.1130	—	5.2019	5.2138	5.1997
100	1.215	—	3.5375	3.5543	3.5381	—	4.3812	4.4205	4.3878
	1.374	—	3.0981	3.1217	3.0989	—	3.7114	3.7852	3.7293
	1.486	—	2.7444	2.7586	2.7285	—	3.1053	3.2048	3.1208

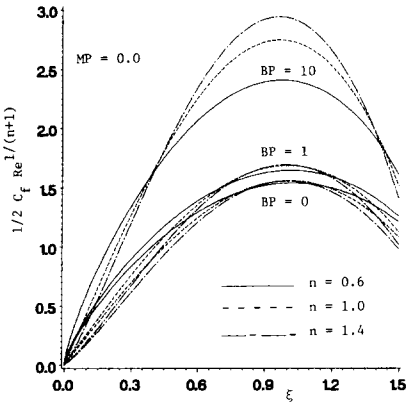

Figure 4 Effects of rotation parameter and viscosity model index on local SFG distribution

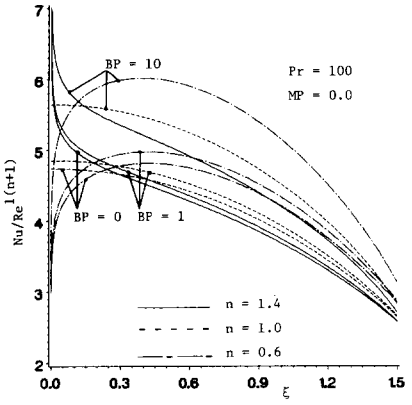

Figure 5 Effects of rotation parameter and viscosity model index on local HTG distribution

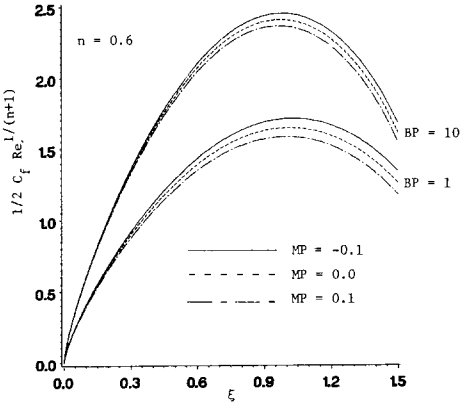

Figure 6(a) Effects of mass transfer and rotation parameters on local SFG distribution for pseudoplastics

which implies that for $\xi \to 0$,

$$\text{HTG} \to \begin{cases} 0 & \text{for } n < 1.0 \\ \infty & \text{for } n > 1.0 \end{cases}$$

Figures 6(a), (b) and 7(a), (b) demonstrate the effect of wall suction/blowing of different fluids on the local skin friction and heat transfer group, respectively. As an extension of Figure 4, Figures 6(a), (b) show that injection reduces and suction increases the SFG slightly. The effect is somewhat less at higher angular velocities. As expected, suction will delay and injection will cause earlier separation when compared with an impermeable (rotating) sphere. The skin friction group is measurably lower for pseudoplastics flowing past rotating spheres ($BP > 1.0$) than for dilatant fluids. SFG values for Newtonian fluids fall between the two graphs (cf. Figures 6(a), (b)). A more dramatic effect of the mass transfer parameter is shown in Figures 7(a), (b), where the local HTG is considered. Following the previously

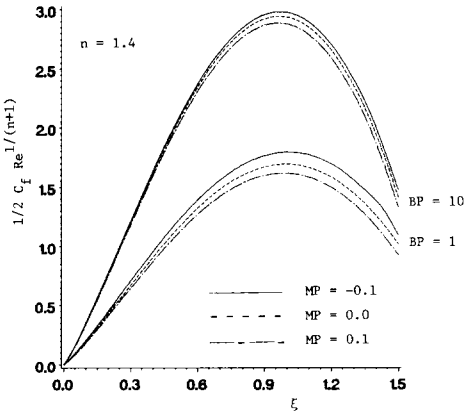

Figure 6(b) Effects of mass transfer and rotation parameters on local SFG distribution for dilatant fluids

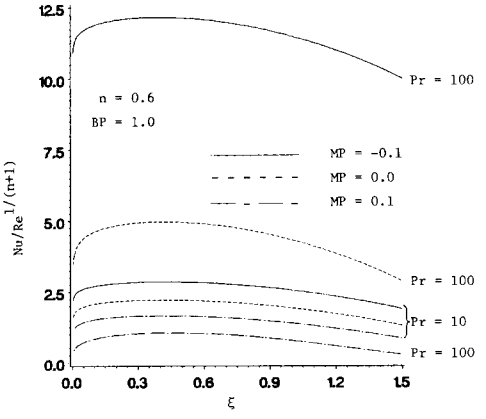

Figure 7(a) Effects of mass transfer parameter and generalized Prandtl number on local HTG distribution for pseudoplastics

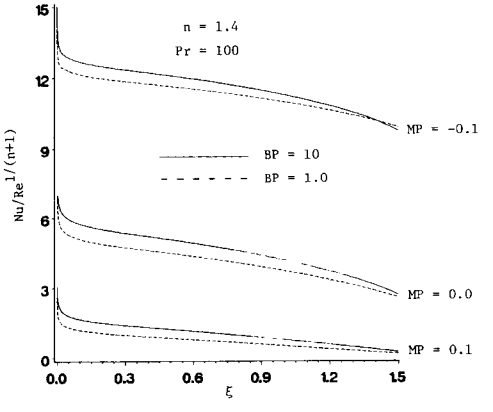

Figure 7(b) Effects of mass transfer and rotation parameters on local HTG distribution for dilatant fluids

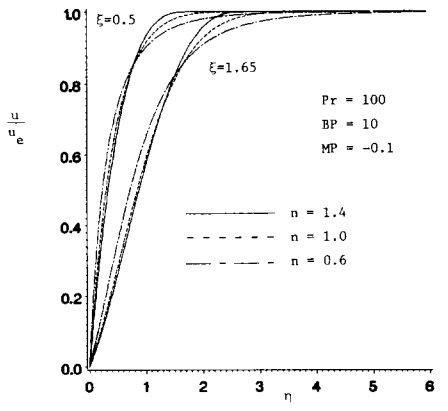

Figure 8(a) Local boundary layer velocity profiles of a rotating sphere with suction immersed in a forced flow field of power-law fluids

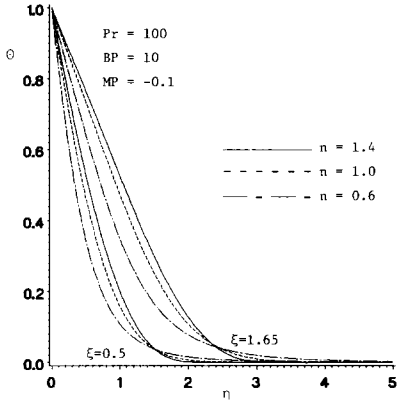

Figure 8(b) Local boundary layer temperature profiles of a rotating sphere with suction immersed in a forced flow field of power-law fluids

discussed trend for pseudoplastics (Figure 7(a)) and dilatant fluids (Figure 7(b)), heat transfer is enhanced via rotation and, more significantly, by withdrawing fluid at temperature T_w from the wall. On the other hand, injection of fluid at $T = T_w$ reduces HTG because the dimensionless wall temperature gradient is less steep when constantly heated fluid is supplied through the wall. As indicated in Figure 7(a), the generalized Prandtl number has a profound effect on the HTG, especially in the presence of suction. The reason is that larger Prandtl numbers imply thinner thermal boundary layers and with suction moving cooler fluid toward the surface, the wall temperature gradient becomes steeper and steeper (cf. Equation 15).

Figures 8(a), (b) show for the suction case the velocity and temperature profiles, respectively, for different fluids at two different positions, i.e., $\xi = 0.5$, which is equivalent to $\phi \approx 30°$ and $\xi = 1.65$ ($\phi \approx 95°$). Both the velocity and thermal boundary layers are thinner for dilatant fluids than for pseudoplastics. Boundary layer separation is eminent for $\xi > 1.65$, since a point of inflection is detectable near $\eta = 0$ (Figure 8(a)) especially for fluids with $n \geqslant 1.0$.

Acknowledgment

This work has been supported in part by the Department of Energy, Office of Basic Energy Science, grant No. DE-FG05-87ER13728.

References

1 Hoskin, N. E. The laminar boundary layer on a rotating sphere. 50 Jahre Grenzschichtforchung , 1955, 127–131
2 Koh, J. C. Y. and Price, J. F. Nonsimilar boundary layer heat transfer of a rotating cone in forced flow. *ASME J. Heat Transfer*, 1967, **89**, 139–145
3 Chao, B. T. and Greif, R. Laminar forced convection over rotating bodies. *ASME J. Heat Transfer*, 1974, **96**, 463–466
4 Lee, M. H., Jeng, D. R., and DeWitt, K. J. Laminar boundary layer transfer over rotating bodies in forced flow. *J. Heat Transfer*, 1978, **100**, 496–502
5 Lien, F. S., Chen, C. K., and Cleaver, J. W. Forced convection over rotating bodies with blowing and suction. *AIAA*, 1986, **24**, 854–856
6 Tsay, S. Y. and Chou, C. H. Laminar convection to rotating disks in non-Newtonian power-law fluids. *Int. Comm. Heat Mass Transfer*, 1983, **10**, 377–383
7 Wang, T.-Y. and Kleinstreuer, C. Laminar free and forced convection of power-law fluids past a horizontal cylinder or sphere. *Int. J. Heat Fluid Flow*
8 Cebeci, T. and Bradshaw, P. *Physical and Computational Aspects of Convective Heat Transfer*. Springer-Verlag, 1984